



High activity and durability of Pt catalyst toward methanol electrooxidation in intermediate temperature alkaline media

Junhua Jiang^{a,*}, Ted Aulich^b

^a Illinois Sustainable Technology Center, University of Illinois at Urbana-Champaign, Champaign, IL 61820, USA

^b Energy and Environmental Research Center, University of North Dakota, Grand Forks, ND 58202, USA

ARTICLE INFO

Article history:

Received 23 January 2012

Accepted 27 February 2012

Available online 5 March 2012

Keywords:

Electrocatalysis

Platinum catalyst

Methanol electrooxidation

Alkaline methanol fuel cell

Intermediate temperature

ABSTRACT

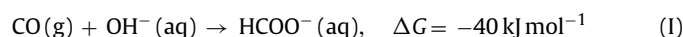
To explore strategies for addressing the CO poisoning of Pt-based catalysts and sluggish anode reaction kinetics which have largely hindered the development of low temperature direct methanol fuel cells, electrocatalytic activity and durability of high-surface Pt toward methanol electrooxidation in alkaline media have been investigated in an intermediate temperature of 80–150 °C by means of voltammetry, chronoamperometry and single cell measurements. In this intermediate temperature range, Pt electrocatalyst is highly active and durable toward the methanol oxidation in alkaline media. Measured exchange current densities are of the order of magnitude of 10^{-7} – 10^{-6} A cm⁻² and sustainable chronoamperometric currents are obtained at potentials as low as 0.16 V vs RHE. An alkaline methanol fuel cell operated at 120 °C using carbon-supported Pt as both anode and cathode electrocatalysts exhibits a peak power density of around 90 mW cm⁻² and provides stable power output under constant current discharge. Accelerated electrooxidation of CO intermediate whose onset is close to that of the methanol electrooxidation and possible reaction of surface CO and hydroxide ions in the intermediate temperature alkaline media are proposed to account for the high activity and durability of Pt. Therefore, the CO-poisoning of Pt-based catalysts and sluggish methanol electrooxidation could be potentially addressed by the use of intermediate temperature alkaline media.

© 2012 Elsevier B.V. All rights reserved.

1. Introduction

The performance of direct methanol fuel cells (DMFCs) based on proton-conducting polymer membranes has been largely limited by sluggish kinetics of anodic methanol oxidation reaction (MOR) in acidic media. Pt has still been the most active single-element electrocatalyst for the MOR [1,2]. However, Pt itself can be easily poisoned owing to the adsorption of reaction intermediates formed during the MOR onto its surfaces. It is well-accepted that CO is the primary surface-blocking species responsible for the poisoning of Pt catalyst [3]. Sustainable activity of Pt for the MOR in acidic media can be accessed only at potentials higher than 0.60 V vs RHE [4,5]. This onset potential for the sustainable MOR has no obvious change even if the temperature is increased to 150 °C [6,7]. Alkaline electrolytes have demonstrated some advantages for the MOR on Pt catalyst, as the onset of the methanol oxidation occurs at lower potential in alkaline media than in acidic media [8–10]. Current efforts are focused on the development of highly active catalysts for accelerated MOR. However, the studies of the MOR in alkaline media have been limited to low temperature. In the low

temperature range, the MOR is not sufficiently facile for the development of high performance alkaline methanol fuel cells (AMFCs) and Pt catalyst still suffers from CO-poisoning. Recently, we have investigated the electrooxidation of small organic molecules in alkaline media in an intermediate temperature range of 80–150 °C [11]. In this intermediate temperature range, CO is likely to spontaneously react with OH⁻ to give formate as follows:



This reaction has been studied as a CO sink on the primitive earth and in the present ocean [12]. The rate of this reaction rate is strongly dependent upon the temperature. The half-time of CO in the gas phase is around 5.5×10^4 years at 25 °C and it is estimated to be decreased to around 1 s at 105 °C. Because formate produced via Reaction (1) is soluble and more electrochemically active than CO on Pt, surface CO formed during the MOR would be readily removed, resulting in considerable decrease in the CO-poisoning of Pt-based catalysts. Moreover, the kinetics of the MOR in alkaline media on Pt has been suggested to be largely determined by the reaction between the surface CO and surface oxygen-containing species (OH), following a Langmuir–Hinshelwood mechanism [13,14]. Accordingly, accelerated electrooxidation of CO intermediate would increase the rate of the MOR.

* Corresponding author. Tel.: +1 217 3335550; fax: +1 217 3338944.
E-mail address: jjjiang@istc.illinois.edu (J. Jiang).

In this work, we have studied the activity and durability of high-surface Pt as a probe of the kinetics of the MOR in alkaline media in the intermediate temperature range. Both high activity and high durability have been observed. Moreover, we have also observed the accelerated CO electrooxidation under the same conditions. We have proposed that the accelerated electrooxidation of CO intermediate and possible chemical reaction of surface CO and hydroxide ions are responsible for the high activity and durability of Pt for the MOR. Finally, high performance intermediate temperature alkaline methanol fuel cell (ITAMFC) has been successfully demonstrated. These facts indicate that the CO-poisoning of Pt-based catalysts and sluggish kinetics of the MOR could be potentially addressed by the use of intermediate temperature alkaline media.

2. Experimental

2.1. Voltammetric and chronoamperometric measurements

All voltammetric and chronoamperometric measurements were performed using a pressurized electrochemical cell based on a modified 300-ml Parr autoclave equipped with a 200 ml Teflon liner [11]. The working electrode was prepared by mechanically depositing high-surface-area Pt black (Alfa, S.A. typically $27 \text{ m}^2 \text{ g}^{-1}$) onto a gold disk electrode of 0.5 mm in diameter, following a powder-rubbing procedure [15]. A 10-cm long platinized Pt wire of 0.5 mm diameter and an Ag/AgCl electrode were used as the counter electrode and the reference electrode respectively. In the following sections, all potentials below were corrected to the RHE scale unless otherwise stated. During the voltammetric measurements with an Autolab general purpose electrochemical system PGSTAT302 (Ecochemie, Netherlands), high-purity nitrogen was introduced into the electrochemical cell to inhibit vaporization of the liquid phase at elevated temperature with gas pressure set at 300 psi unless otherwise stated. All solutions were prepared from methanol (>99.9%, Aldrich) or KOH (>85%, Aldrich) with deionized water with a resistivity of $18.2 \text{ M}\Omega \text{ cm}$. All voltammetric and chronoamperometric measurements for the MOR were carried out in $0.5 \text{ mol dm}^{-3} \text{ KOH} + 0.5 \text{ mol dm}^{-3} \text{ methanol}$. To investigate the electrochemical oxidation of CO, high purity CO was introduced into the electrochemical cell with the pressure set at 300 psi.

2.2. Characterization of high surface Pt electrode

The real electrochemical surface area of the Pt black layer coated onto the Au disk was assessed using underpotential deposited (upd) hydrogen and Cu stripping techniques [16,17]. The upd Cu was adsorbed onto the electrode surface by polarizing it at 0.30 V vs RHE for 30 min in a $0.5 \text{ mol dm}^{-3} \text{ H}_2\text{SO}_4$ containing $0.020 \text{ mol dm}^{-3} \text{ CuSO}_4$. The potential was then scanned positively at 10 mV s^{-1} . The resulting current was integrated after correcting for the contribution of oxide growth and double layer charging currents. The electrochemical surface area was calculated to be 5.9 cm^2 and 5.8 cm^2 measured from the upd hydrogen and Cu stripping, respectively, lower than its physical surface area (ca. 7.3 cm^2) estimated from its BET specific area and the mass of the Pt layer. The latter was measured by dissolving Pt black layer in boiling aqua regia, followed by removing the excess and measuring inductively coupled plasma-atomic emission spectroscopy (ICP-AES) spectra. A value of around $2.7 \times 10^{-5} \text{ g}$ was obtained, corresponding to a Pt loading of 13.5 mg cm^{-2} .

All currents were corrected for the geometrical surface area of the Pt-coated Au disk electrode unless otherwise stated. Intrinsic current densities were corrected to the electrochemical real surface area. The mass activities of the catalyst were calculated from

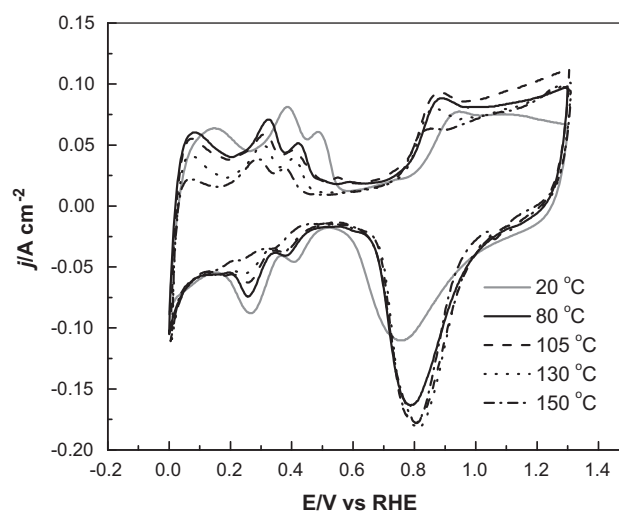


Fig. 1. Cyclic voltammograms for a Pt black coated Au disk electrode in $0.5 \text{ mol dm}^{-3} \text{ KOH}$ at 50 mV s^{-1} as a function of reaction temperature.

measured chronoamperometric pseudo steady-state currents and the catalyst mass.

2.3. Single cell measurements

The measurements of fuel cell performance were performed using a 5-cm^2 testing cell and a lab-constructed control system. Carbon supported Pt (60 wt%) catalyst was obtained from Fuel Cell Store. The Pt/C catalyst was inked using the mixture of ethanol and ethylene glycol under ultrasonic stirring and the resulted ink was introduced onto the carbon-cloth diffusion layer via a brush-painting procedure until a loading of 4 mg cm^{-2} Pt was obtained. The alkaline electrolyte membrane was prepared by immersing polybenzimidazole-based membrane (Fumapem® AA, FuMA-Tech GmbH) of around $40 \mu\text{m}$ in thickness in $10 \text{ mol dm}^{-3} \text{ KOH}$ solution overnight. The membrane-electrode-assemblies (MEAs) were prepared by sandwiching the anode catalyzed diffusion layer, the alkaline electrolyte membrane and the cathode catalyzed diffusion layer under 400 lb cm^{-2} and at room temperature. During single cell measurements, pure oxygen was supplied to the cathode side at 160 SCCM without external humidification. An aqueous solution of $2 \text{ mol dm}^{-3} \text{ CH}_3\text{OH}$ and $2 \text{ mol dm}^{-3} \text{ KOH}$ was pumped through the anode chamber at a flow rate of 6 ml min^{-1} using a constant pressure liquid pump (Chrom Tech, Inc.). A pressure of 30 psi was applied to inhibit the vaporization of the aqueous phase. The cell voltage-current curves were measured using an Autolab general purpose electrochemical system PGSTAT302 integrated with a 20 A current booster.

3. Results and discussion

Base cyclic voltammograms for a Pt black coated Au disk electrode in $0.5 \text{ mol dm}^{-3} \text{ KOH}$ solution as a function of temperature are shown in Fig. 1. Analogous to literature results [18], three characteristic zones corresponding to hydrogen electrochemistry, double layer and oxygen electrochemistry are observed. The peak potentials associated with hydrogen adsorption/desorption in the hydrogen electrochemistry zone over 0 to around 0.50 V are negatively shifted as the temperature is increased, accompanied by obvious decrease in the peak currents at higher temperature. In the oxygen electrochemistry zone over 0.65 to approximately 1.3 V, the value of the cathode peak current is initially increased when the temperature is increased from 20 to $80 \text{ }^\circ\text{C}$. Further increasing temperature has no obvious influence on the peak currents.

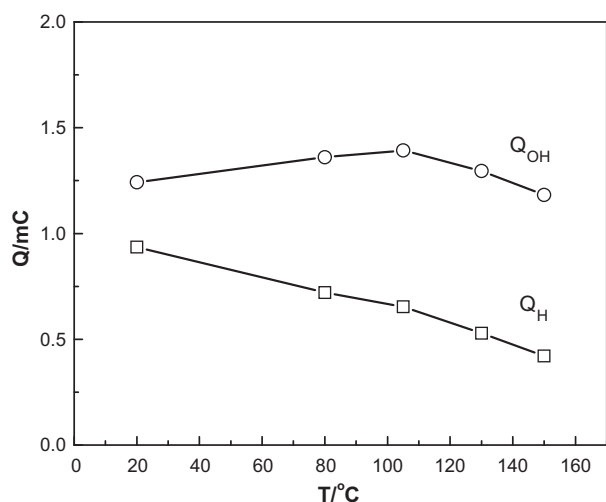


Fig. 2. Temperature dependence of hydrogen adsorption/desorption charge (Q_H) and oxygen desorption charge (Q_{OH}) with data taken from Fig. 1.

Fig. 2 shows the temperature dependence of the hydrogen adsorption/desorption charge (Q_H) and the oxygen-containing species desorption charge (Q_{OH}). Q_H can be determined via $Q_H = 0.5(Q_{total} - Q_{dl})$, where Q_{total} and Q_{dl} are the charge surrounded by the hydrogen adsorption/desorption curve in the potential range of 0–0.50 V and the capacitive charge due to double layer charging, respectively. Q_{OH} can be calculated from the charge associated with the reduction peak in the potential range of 0.6–1.2 V during the negative-going scans. Interestingly, it is clear that Q_H is decreased while Q_{OH} has no obvious changes when the temperature is increased from 20 to 150 °C. The decrease of Q_H with increasing temperature suggests that the surface area corresponding to the hydrogen adsorption/desorption is significantly decreased at higher temperatures. Only 45% of its original surface area remains active when the temperature is increased to 150 °C. However, the minor influence of increasing temperature on Q_{OH} indicates that there is no obvious decrease in the electrode surface area for the adsorption/desorption of oxygen-containing species. The difference between the temperature dependence of Q_H and Q_{OH} could be understood that the hydrogen adsorption/desorption is more sensitive to the adsorption of impurities onto the electrode surfaces, which is normally increased with increasing temperature. For the convenience of discussion in the following sections, it is assumed that the variations of the surface area for the MOR as a function of reaction temperature are insignificant based on the temperature dependence of Q_{OH} .

The intrinsic activity (j_s) of Pt catalyst toward the methanol oxidation in intermediate temperature alkaline media as a function of reaction temperature measured at 10 mV s⁻¹ is shown in Fig. 3. It is clearly seen that Pt is more active with increasing temperature. At 80 °C, Pt is active at potentials higher than 0.25 V. This value is decreased to approximately 0.10 V when the temperature is increased to 130 °C. The intrinsic activity of Pt catalyst is measured to be around 0.06 mA cm⁻² at 0.21 V and at this temperature, corresponding to a turnover frequency of around 5 s⁻¹. This turnover frequency suggests that the oxidation of a monolayer methanol could be completed in around 0.1 s assuming a single site adsorption model [19]. Compared to literature results reported for the Pt activity toward the methanol oxidation in acidic media [6,20], Pt catalyst is much more active in intermediate temperature alkaline media. In acidic media and at 60 °C, nanostructured Pt demonstrates the sustainable activity to the methanol oxidation at around 0.38 V with a specific activity of around 0.42 μA cm⁻² [20]. Further increasing temperature cannot effectively increase the Pt activity

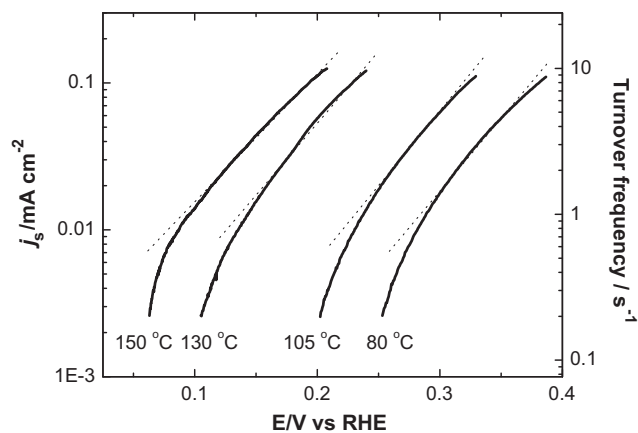


Fig. 3. Intrinsic activity (j_s) of a Pt black coated Au disk electrode in 0.5 mol dm⁻³ KOH + 0.5 mol dm⁻³ CH₃OH measured using a linear potential scan at 10 mV s⁻¹ as a function of reaction temperature.

Table 1

Tafel slopes (b) and exchange current density (j_o) for the electrooxidation of 0.5 mol dm⁻³ methanol in 0.5 mol dm⁻³ KOH on a Pt black coated Au disk electrode as a function of reaction temperature.

Temperature (°C)	b (mV dec ⁻¹)	$10^7 \times j_o$ (A cm ⁻³)
80	133	1.0
105	128	3.3
130	111	7.1
150	118	23.6

in acidic media. The onset of the sustainable methanol oxidation commences at around 0.60 V even if the temperature is increased to 150 °C [6]. Therefore, it is reasonably envisioned that Pt could be one hundred times more active at low potentials in intermediate temperature alkaline media than in acidic media.

The values of the exchange current density (j_o) are obtained by extrapolating the Tafel lines to the equilibrium potential (E_{eq}) for the MOR, whose value is 0.016 V vs RHE at each temperature. The j_o values corrected to the real electrochemical surface area as a function of reaction temperature are listed in Table 1. The orders of magnitude of j_o range from 10⁻⁷ to 10⁻⁶ A cm⁻² in the intermediate temperature range. An Arrhenius plot of the j_o values is shown in Fig. 4. If j_o is expressed as $j_o = A \exp(-E_a/RT)$ where E_a is the activation energy and other terms have their normal meanings, a weighed

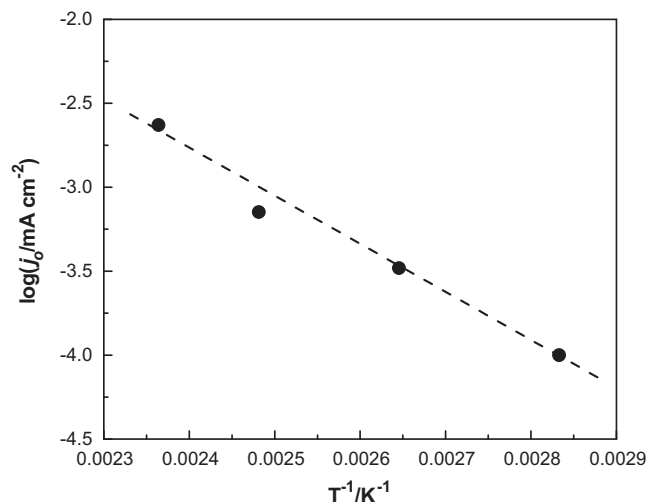


Fig. 4. Arrhenius plot of exchange current density.

least square fit to the data gives $E_a = 53.6 \pm 5.3 \text{ kJ mol}^{-1}$. This value is consistent with literature data which fall within a range of $24\text{--}76 \text{ kJ mol}^{-1}$ measured for the electrooxidation of 0.5 mol dm^{-3} CH_3OH in alkaline media [12,4]. Cohen et al. measured the E_a values under different electrode conditions and summarized the factors affecting the magnitude of the calculated E_a [4]. These include surface poisoning from methanol oxidation intermediates, anion adsorption from the electrolyte, pH effects and surface oxide formation. Tripkovic et al. demonstrated that the values of E_a are dependent upon the chemical composition of electrodes: 46.5 kJ mol^{-1} for Pt, 45.5 kJ mol^{-1} for Pt_2Ru_3 and 40.6 kJ mol^{-1} for Pt_3Ru_2 [12]. Here, the E_a value was calculated from the values of the exchange current density. The influences of those factors proposed by Cohen et al. could be decreased. Therefore, it should be a more realistic indication of the temperature dependence of the rate constant for the MOR reaction.

The values of the Tafel slopes measured from linear portions of a log current density vs potential plot (Fig. 3) are listed in Table 1. They are in range of $111\text{--}133 \text{ mV dec}^{-1}$ in the intermediate temperature range, in agreement with literature data for the MOR in alkaline media on platinized [8] and single crystal Pt electrodes [21–23]. Tripkovic et al. proposed that the chemical reaction between the surface intermediate CO_{ad} and OH_{ad} is the rate-determining step and the overall rate equation for the MOR could be written as follows [22]:

$$j = kc_{\text{CH}_3\text{OH}}^{0.5}c_{\text{OH}^-}^{0.5} \exp\left(\frac{\alpha F}{nF}\eta\right) \quad (1)$$

where k is a constant and other terms have their normal meanings. From this expression a Tafel slope ranging from 120 to 164 mV dec^{-1} as the temperature is increased from 20 to 150°C could be obtained. However, several factors including electrode surface structure, pH values, surface absorbates and their interactions affect measured Tafel slopes. Spendelow et al. studied the influences of preadsorbed CO on the MOR at room temperature and reported that the measured Tafel slopes vary from 100 to 120 mV dec^{-1} [21], depending on the coverage of pre-adsorbed CO. The value is close to 120 mV dec^{-1} on Pt single crystal electrodes [22,23]. On a platinized Pt electrode, the Tafel slope is around 110 mV dec^{-1} for the MOR in NaOH solution, but it is changed to around 200 mV dec^{-1} in the carbonate and bicarbonate media [8]. Therefore, our Tafel slopes which can be fitted using Eq. (1) indicate that the methanol oxidation in alkaline media at low temperature and in the intermediate temperature range is highly likely to follow a similar reaction mechanism.

To evaluate the activity durability of Pt catalyst at temperature relevant to the operation of the intermediate temperature alkaline methanol fuel cells, current–time transients are measured at 130°C by stepping potential from 0V where no methanol oxidation occurs to a given potential where the methanol oxidation is triggered for 300 s , as shown in Fig. 5. The common features of the current–time transients are characterized by fast current drops in around 10 s followed by pseudo steady-state currents at longer time. The changes of the pseudo steady-state currents with reaction time are dependent upon the potential. We characterize these changes by performing a linear regression on the data starting 10 s after the polarization and continuing for the rest of the experiment. The resulting current decay is normalized by dividing by the average current over the measurement period and multiplied by one hundred to obtain a rate of poisoning, which is the rate of current decay in $\% \text{ min}^{-1}$. The variation of the decaying rate as a function of potential is shown in Fig. 6. At 0.11 V , the electrode is easily deactivated at a current-loss rate of $20\% \text{ min}^{-1}$. Increasing the potential substantially decreases the poisoning rate. Interestingly, the electrode provides reasonably stable activity at 0.21 V . At this potential and higher, the decay rate remains very low, although at higher

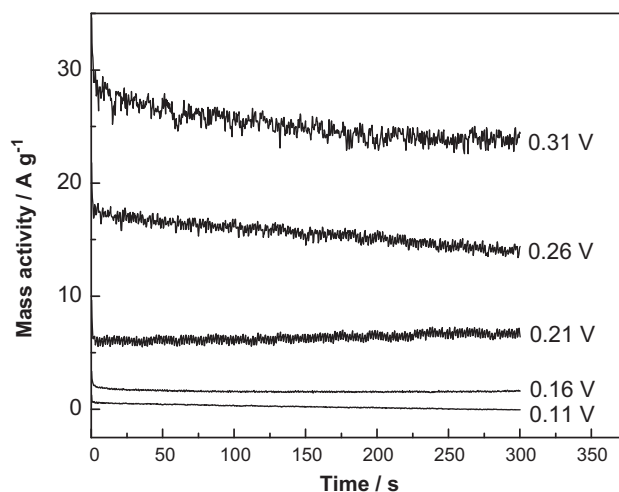
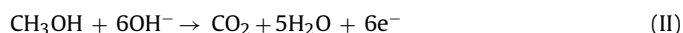


Fig. 5. Current–time transients for a Pt catalyst coated Au disk electrode in 0.5 mol dm^{-3} $\text{KOH} + 0.5 \text{ mol dm}^{-3}$ CH_3OH measured at 130°C after stepping potential from 0V to a given potential for 300 s of polarization.

potentials there is a slight increase in decay rate. The mass activity of the Pt catalyst is characterized by a value of 7.0 A g^{-1} at 0.21 V and 130°C , around 50 times higher than a literature value of 0.15 A g^{-1} at 0.38 V and 60°C measured for the nanostructured Pt toward the MOR in acidic media [20].

It is interesting to explore the origins of the high activity and durability of Pt for the MOR in intermediate temperature alkaline media. In acidic media, the MOR follows a so-called dual-path mechanism involving reactive intermediate in the direct path and surface blocking species in the indirect path [8,21]. Adsorbed CO has long been considered as the only surface blocking species [3]. The surface CO can strongly bind to Pt and lead to severe limitations in the oxidation kinetics, resulting in significant polarization loss. The oxidative removal of the surface CO requires a potential more positive 0.6 V vs RHE. In alkaline media, the anodic oxidation of methanol can be written as:



This reaction has been suggested to proceed through an adsorbed CO intermediate which is formed in Reaction (III) [21].

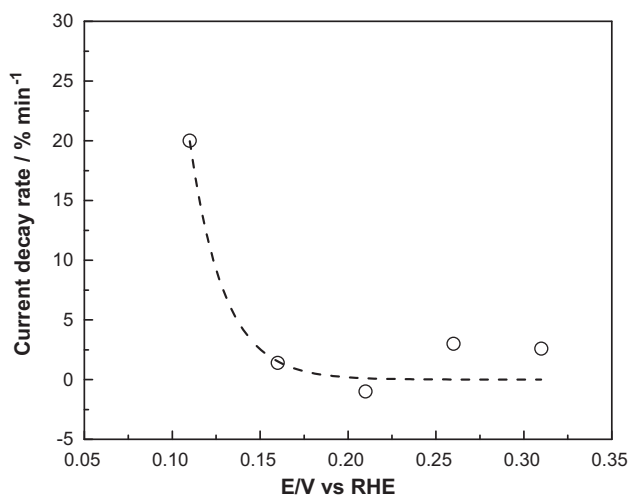
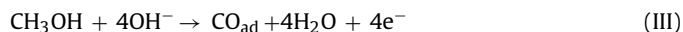


Fig. 6. Dependence of current decay rates in chronoamperometric measurements on applied potential with data extracted from Fig. 4 ignoring first 10 s .

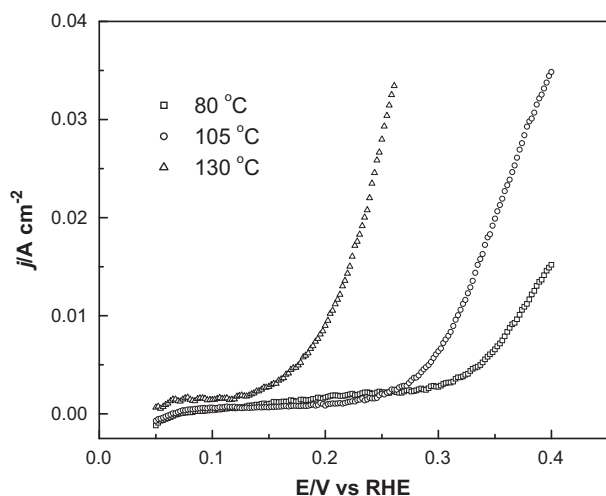


Fig. 7. Temperature dependence of polarization curves for a Pt black coated Au disk electrode in 0.5 mol dm^{-3} KOH equilibrated with 300 psi CO measured at a scan rate of 10 mV s^{-1} .

Adsorbed CO is subsequently oxidized to CO_2 via a Langmuir–Hinshelwood type of reaction [12]:



Adsorbed OH in Reaction (IV) is formed by the discharge of hydroxide ions, as described below:



At low temperature, the methanol oxidation can proceed at low potential but the process is rapidly poisoned by the accumulation of CO (Reaction (III)) which is not readily oxidized. Several groups have provided the measurements of CO coverage during or after the methanol oxidation by voltammetric oxidation of CO in methanol-free solution [21,24]. CO was also detected during the methanol oxidation using IR spectroscopy [25]. It is therefore postulated that accelerating the kinetics of the oxidation of adsorbed CO intermediate (Reaction (IV)) is likely to increase the overall rate of the methanol oxidation and to decrease the CO-poisoning of the electrode.

To verify this postulation, we have studied the electrooxidation of bulk CO in the intermediate temperature alkaline media. Fig. 7 shows the current–potential curves measured by a linear potential scan at 10 mV s^{-1} as a function of reaction temperature. It is clearly seen that the onset potentials of the CO oxidation are shifted negative with increasing temperature. At 80°C , the onset of the CO oxidation occurs at around 0.30 V . This potential is negatively shifted to around 0.13 V as the temperature is increased to 130°C . These onset potentials are very close to those for the MOR under the similar conditions. This strongly suggests that simultaneous oxidation of CO and methanol is possible at potentials not far from their onset potentials. Therefore, the chance for the surface CO accumulation on Pt during the MOR is low. Additionally, the chemical reaction of CO and hydroxide (Reaction (I)) in the intermediate temperature range would facilitate the removal of surface CO since the product formate is soluble and more electrochemically active than CO. Fig. 5 demonstrates that the sustainable currents for the MOR are obtained even at potentials as low as 0.16 V . It is therefore expected that the CO-poisoning of Pt-based catalysts could be potentially addressed by the use of intermediate temperature alkaline media.

In alkaline media, progressive carbonation of the solution caused by CO_2 produced during the MOR may decrease the pH value of the solution close to the electrode surface, has been proposed to

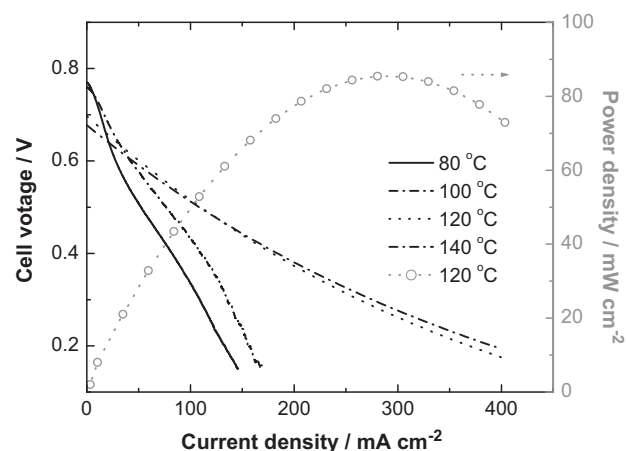


Fig. 8. Temperature dependence of cell voltage–current density curves for a single ITAMFC using Pt/C as both anode and cathode electrocatalysts and the dependence of power density on current density for the curve measured at 120°C .

be responsible for the chronoamperometric current decays [26,27]. We have estimated the limiting current value for the MOR on the Pt electrode by assuming 6 electrons transferred per methanol molecule and a diffusion efficient of $5 \times 10^{-5} \text{ cm}^2 \text{ s}^{-1}$ under our conditions. A value of around $1.5 \times 10^{-3} \text{ A}$ (corresponding to a mass activity of 56 Ag^{-1} in Fig. 5) is obtained. The measured current densities at 0.26 V and 0.31 V are $4.5 \times 10^{-4} \text{ A}$ and $7.5 \times 10^{-4} \text{ A}$ respectively. Therefore, the slow current decays measured at 0.26 V and 0.31 V in Fig. 5 are likely to be caused by the mass transport limitation although the contribution of the progressive carbonation cannot be ruled out.

The activity and durability of the Pt catalyst are further studied in a realistic intermediate temperature alkaline methanol fuel cell (ITAMFC) using carbon supported Pt as both the anode and cathode electrocatalysts. We have studied the influences of the concentrations of both methanol and KOH on the cell performance. The optimized values are 2 mol dm^{-3} CH_3OH and 2 mol dm^{-3} KOH. During all single cell studies, an aqueous solution of 2 mol dm^{-3} $\text{CH}_3\text{OH} + 2 \text{ mol dm}^{-3}$ KOH was fed to the anode chamber. The performance of the ITAMFC single cell as a function of reaction temperature is shown in Fig. 8. The values of the open-circuit potential (OCP) are in the range of $0.68\text{--}0.75 \text{ V}$, lower than the theoretical value of around 1.2 V [28]. Moreover, the OCP values slightly decrease with increasing temperature. The lower OCP values and their temperature dependence are likely to be caused by methanol crossover from the anode side to the cathode side. Interestingly, substantial cell performance improvement has been observed when the temperature is increased from 100 to 120°C . The cell performance measured at 140°C is very close to that at 120°C . This temperature dependence of the cell performance suggests that an optimized operating temperature could fall within $120\text{--}140^\circ\text{C}$. These facts would be important for the development of high performance DMFCs. In acidic media, it is less likely to use single-element Pt as the anode electrocatalyst and the introduction of Ru to Pt has partially addressed the CO-poisoning of the catalyst and has improved the catalyst activity [29,30]. However, these achievements are not sufficient to support the development of high performance DMFCs. Moreover, the leaching of Ru from bimetallic PtRu anode catalysts has been raised as a potential issue for traditional DMFCs. These challenges could be potentially addressed by the development of the ITAMFC. It is expected that the performance of the ITAMFCs will be further improved by the development of the alkaline electrolyte membranes with decreased methanol crossover and increased conductivity.

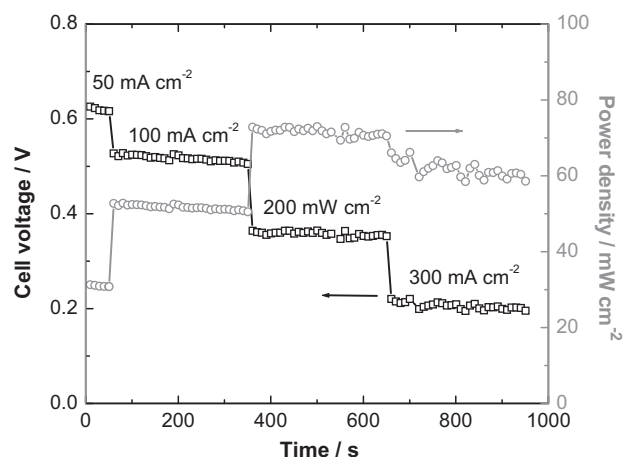


Fig. 9. Dependence of cell voltage and power density on discharging time upon applying a four-step constant current for a single ITAMFC operated at 120 °C.

The dependence of power density measured at 120 °C as a function of discharge current density is also provided in Fig. 8. The peak power density seen at around 280 mA cm⁻² reaches 90 mW cm⁻². This peak power density is obviously higher than literature data which are normally around 50 mW cm⁻² for traditional DMFCs [31,32]. For a high temperature DMFC based on phosphoric acid PBI membrane, the peak power density was limited to 12–16 mW cm⁻² at 175 °C [33]. Therefore, higher power output would be one of obvious advantages for the ITAMFC over traditional DMFCs.

The durability of Pt catalyst in the ITAMFC is evaluated in a constant current discharge model. The variations of cell voltage and power density with discharge time upon applying a four-step constant current are shown in Fig. 9. At 50 mA cm⁻², the cell voltage remains stable at around 0.62 V and the corresponding power output is 32 mW cm⁻². At 100 mA cm⁻², the cell voltage remains stable at around 0.52 V and the corresponding power output is 52 mW cm⁻². At 200 mA cm⁻², the cell voltage and power output slightly vary around 0.36 V and 72 mW cm⁻², respectively. Further increasing current density to 300 mA cm⁻² slightly decreases the cell voltage and power output to 0.20 V and 60 mW cm⁻², respectively. These discharge characters strongly suggest that the activity of the single element Pt anode electrocatalyst is durable in the ITAMFC and could meet the requirement of providing stable power output even under a reasonably high current discharge. This would be important for the application of ITAMFC as a portable power source. Moreover, the stable cell voltages measured under constant-current discharge suggest that the poisoning of Pt/C catalysts at the anode side can be neglected. Because the CO-poisoning of the anode catalysts has considerably plagued the commercialization of traditional DMFCs, the minimized CO-poisoning of Pt in our case is another obvious advantage of the ITAMFC.

4. Conclusions

High activity and durability of high-surface Pt catalyst toward the MOR in intermediate temperature alkaline media indicate that

the CO poisoning of Pt-based catalysts and sluggish kinetics of the MOR at the anode side of direct methanol fuel cells could be potentially addressed by the use of intermediate temperature alkaline media. The ITAMFC has the potential to provide low-cost power sources for a range of applications since it is possible to replace Pt using non-Pt catalysts in the alkaline fuel cell system for decreased cost without obvious performance decrease. Because it utilizes alcohols as fuel, there is no need of hydrogen infrastructure and it can provide constant power output longer than battery. It is also one of potential technologies for transportation applications. The challenge associated with the carbonation of the alkaline electrolyte could be potentially addressed through the use of recirculating alkaline fuels and anion-exchange membrane electrolytes. It is expected that high-performance and low-cost ITAMFC technology can be achieved via the development of more active non-Pt catalysts, higher performance alkaline membranes and engineering controls.

References

- [1] D. Zurawski, M. Wasberg, A. Wieckowski, *J. Phys. Chem.* 94 (1990) 2076–2082.
- [2] M. Bergelin, E. Herrero, J.M. Feliu, M. Wasberg, *J. Electroanal. Chem.* 467 (1999) 74–84.
- [3] C. Lamy, J.M. Leger, S. Srinivasan, in: J.O'M. Bockris, B.E. Conway, R.E. White (Eds.), *Modern Aspects of Electrochemistry*, vol. 34, 2001, pp. 53–118.
- [4] J. Cohen, D. Volpe, H. Abruna, *Phys. Chem. Chem. Phys.* 9 (2007) 49–77.
- [5] E.A. Batista, I. Iwasita, W. Vielstich, *J. Phys. Chem. B* 108 (2004) 14216–14222.
- [6] H. Nonaka, Y. Matsumura, *J. Electroanal. Chem.* 520 (2002) 101–110.
- [7] H. Nonaka, Y. Matsumura, *J. Chem. Eng. Jpn.* 35 (2002) 626–633.
- [8] E. Yu, K. Scott, R. Reeve, *J. Electroanal. Chem.* 547 (2003) 17–24.
- [9] J. Prabhuram, R. Manoharan, *J. Power Sources* 74 (1998) 54–61.
- [10] J. Spindelov, G. Lu, P. Kenis, A. Wieckowski, *J. Electroanal. Chem.* 568 (2004) 215–224.
- [11] J. Jiang, T. Aulich, in: Y. Shao (Ed.), *Electrochemical Cells*, InTech, 2012, pp. 161–178.
- [12] J. van Trump, S. Miller, *Earth Planet. Sci. Lett.* 20 (1973) 145–150.
- [13] A. Tripkovic, S. Strbac, K. Popovic, *Electrochim. Commun.* 5 (2003) 484–490.
- [14] A. Khan, R. Ahmed, M. Mirza, *Nucleus* 44 (2007) 133–141.
- [15] A. Kucernak, J. Jiang, *Chem. Eng. J.* 93 (2003) 81–90.
- [16] J. Jiang, A. Kucernak, *Chem. Mater.* 16 (2004) 1362–1367.
- [17] C.L. Clair, A. Kucernak, *J. Phys. Chem. B* 106 (2002) 1036–1047.
- [18] T.J. Schmidt, P.N. Ross, N.M. Markovic, *J. Phys. Chem. B* 105 (2001) 12082–12086.
- [19] T. Iwasita, F.C. Nart, *J. Electroanal. Chem.* 317 (1991) 291–298.
- [20] J. Jiang, A. Kucernak, *J. Electroanal. Chem.* 533 (2002) 153–165.
- [21] J. Spindelov, A. Wieckowski, *Phys. Chem. Chem. Phys.* 9 (2007) 2654–2675.
- [22] A. Tripkovic, K. Popovic, J. Lovic, V. Jovanovic, A. Kowal, *J. Electroanal. Chem.* 572 (2004) 119–128.
- [23] A. Tripkovic, K. Popovic, J. Momcilovic, D. Drazic, *J. Electroanal. Chem.* 418 (1996) 9–20.
- [24] E. Morallon, F. Cases, J. Vazquez, A. Aldaz, *Electrochim. Acta* 37 (1992) 1883–1886.
- [25] J. Perez, E. Munoz, E. Morallon, F. Cases, J. Vazquez, A. Aldaz, *J. Electroanal. Chem.* 368 (1994) 285–291.
- [26] K. Matsuoka, Y. Iriyama, T. Abe, M. Matsuoka, Z. Ogumi, *Electrochim. Acta* 51 (2005) 1085–1090.
- [27] C. Lamy, E.M. Belgsir, J.M. Leger, *J. Appl. Electrochem.* 31 (2001) 799–809.
- [28] J. Larminie, A. Dicks, *Fuel Cell Systems Explained*, second ed., Wiley, England, 2003, p. 143.
- [29] M. Koper, J. Lukkien, A. Jansen, R.A. van Santen, *J. Phys. Chem. B* 103 (1999) 5522–5529.
- [30] J. Jiang, A. Kucernak, *J. Electroanal. Chem.* 543 (2003) 187–199.
- [31] L. Han, C. Song, L. Zhang, J. Zhang, H. Wang, D. Wilkinson, *J. Power Sources* 155 (2006) 95–110.
- [32] E. Reddington, A. Sapienza, B. Gurau, R. Viswanathan, S. Sarangapani, E.S. Smotkin, *Science* 280 (1998) 1735–1737.
- [33] M. Mamlouk, K. Scott, N. Hidayati, *J. Fuel Cell Sci. Eng.* 8 (2011) 069009/1–069009/69009.